Proceedings of the 30th International Cosmic Ray Conference
Rogelio Caballero, Juan Carlos D'Olivo, Gustavo Medina-Tanco,
Lukas Nellen, Federico A. Sánchez, José F. Valdés-Galicia (eds.)
Universidad Nacional Autónoma de México,
Mexico City, Mexico, 2008
Vol. 1 (SH), pages 857–860

30TH INTERNATIONAL COSMIC RAY CONFERENCE

The transport and acceleration of anomalous cosmic rays in the inner heliosheath

S.E.S. FERREIRA[1], M.S. POGIETER[1] AND K. SCHERER[2].
[1]*Unit for Space Physics, School of Physics, North-West University, 2520 Potchefstroom, South Africa*
[2]*Institut für Theoretische Physik, Lehrstuhl IV: Weltraum- und Astrophysik, Ruhr-Universität Bochum, D-44780 Bochum, Germany*
Stefan.Ferreira@nwu.ac.za

Abstract: The transport and acceleration of anomalous cosmic rays in the inner heliosheath is studied. A unique numerical model is used to calculate the interaction of the solar wind and the local interstellar medium, neutral hydrogen and pickup ions hydrodynamically. The divergence of the flow, heliospheric magnetic field and Alfven speed are calculated and then inserted into a transport part which calculates cosmic ray transport and acceleration for this realistic heliosphere. We show that adiabatic heating and stochastic acceleration plays a major role in explaining Voyager 1 observations both at the termination shock and in the inner heliosheath. While the inclusion of adiabatic heating in a numerical modulation model results in the correct spectral shape of accelerated anomalous particles for energies $\leq\sim$ 10 MeV at the termination shock, stochastic acceleration effectively accelerates these particles further out into the inner heliosheath. These accelerated particles are then modulated back inwards resulting in realistic radial gradients as well as an upturn in the computed spectra.

Introduction

The recent crossing [1, 2] of the termination shock, and the entering into the inner heliosheath by the Voyager 1 spacecraft, has provided new challenges for numerical models describing cosmic ray particle transport and acceleration in this region [3]. For example, the anomalous cosmic ray observations by Voyager 1, e.g. [1], show that the peak in the particle intensity is not at the shock but rather seems to be a few AU beyond, well into the inner heliosheath. These observations have led modelers to include previously neglected acceleration mechanisms into numerical models. First, the compression of the post shocked plasma due to charge exchange [4, 5] results in effective adiabatic acceleration (heating) in the inner heliosheath [6, 7]. Second, there may also be acceleration of a stochastic nature [8, 9] as recently modelled by [10] and [11].

In this work we focus on stochastic and adiabatic acceleration of anomalous cosmic rays in the inner heliosheath. The effects of stochastic acceleration only on anomalous cosmic rays were illustrated by [10] and adiabatic acceleration only by [6], [7] and [12], while [11] included both these processes in one model.

Different from previous studies is that we will use our unique model [13, 14] to compute the interaction of the solar wind and the local interstellar medium, neutral hydrogen and pickup ions to calculate the heliospheric interface and plasma flow inside. From this the divergence of the flow can be calculated more realistically than used by e.g. [11] and [10] who assumed an analytical expression for the solar wind flow. From the flow profiles the heliospheric magnetic field is calculated in the kinematic approximation [7]. The computed density profile and magnetic field are then used to calculate the Alfven speed much more realistically than [11] and [10] where both used analytical expressions based on a Parker field. The calculated flow profiles, magnetic field and Alfven speed are then inserted into a transport part that calculates cosmic ray transport and acceleration in this realistic heliosphere.

Model and Parameters

For the interaction between various fluids the Euler equations are solved. The plasma flow is then used in a magnetic part where the induction equation is solved. For details see [7]. The flow profiles and magnetic field are then used in a transport part, based on solving the transport equation [15]

$$\frac{\partial f}{\partial t} = -\left(\vec{V} + \langle v\vec{_D} \rangle\right) \cdot \nabla f + \nabla \cdot (\vec{K}_S \cdot \nabla f) + \frac{1}{3}(\nabla \cdot \vec{V}) \frac{\partial f}{\partial \ln P} + \frac{1}{P^2} \frac{\partial}{\partial P}(P^2 D \frac{\partial f}{\partial P}) + Q \quad (1)$$

in two spatial dimensions (r, θ) with θ the polar angle, r the radial distance and t the time, P is rigidity, Q is any particle sources inside the heliosphere and $\vec{V}$ is the solar wind velocity. In Equation 1, $\vec{K_S}$ is the diffusion tensor and $\langle v\vec{_D} \rangle$ the averaged guiding center drift velocity for a near isotropic distribution function f.

The two energy terms in Equation 1 are important. Concerning the first, when $\nabla \cdot \vec{V} > 0$ the cosmic rays are adiabatically cooled which generally occurs inside the termination shock. For $\nabla \cdot \vec{V} < 0$, cosmic rays are accelerated via diffusive shock acceleration at the termination shock. In the inner heliosheath, for most of the downstream region, the solar wind is compressed due to charge exchange [4, 5] resulting in $\nabla \cdot \vec{V} < 0$ and adiabatic heating occurs [6]. Second, acceleration of a stochastic nature [8, 9, 10, 11] has been known to exist and be present in turbulent downstream shocks. This can be included in Equation 1 by specifying an approximated momentum diffusion coefficient D [16] given by

$$D = D_0 \frac{P^2 V_A^2}{9 K_{||}} \quad (2)$$

with V_A the Alfven speed and D_0 a constant and $K_{||}$ the parallel mean free path. Furhtermore

$$V_A = \frac{B}{\sqrt{\mu_0 \rho}} \quad (3)$$

with ρ the solar wind density. As shown by e.g. [10] the Alfven speed in the upstream region of the termination shock is relative small resulting in almost no stochastic acceleration of cosmic rays. However, in the heliosheath region B abruptly increases over the termination shock by a factor corresponding to the compression ratio. Further into the heliosheath a steady increase is computed due to the decelerating plasma. According to Equation 3 this results in an increase in the Alfven speed V_A and stochastic acceleration in the inner heliosheath becomes quite viable.

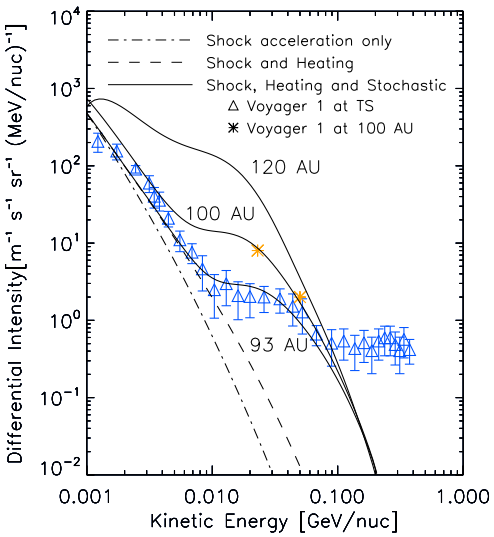

Figure 1: Computed spectra for singly-ionized anomalous He at the termination shock (93 AU) for three acceleration scenarios: (1) diffusive shock acceleration only (dashed-dotted line), (2) diffusive shock acceleration and adiabatic heating (dashed line) and (3) shock acceleration, heating in the inner heliosheath and acceleration of a stochastic nature (solid lines). The latter scenario is shown at the shock (bottom solid line), at 100 AU and at 120 AU (top solid line). In comparison the observed Voyager 1 spectra at the observed termination shock are shown as the triangles [10, 17]. Also shown by the asterisk symbols are Voyager 1 observations at 100 AU (http://voycrs.gsfc.nasa.gov).

Discussion

Figure 1 shows computed spectra for singly-ionized anomalous He at the termination shock (93 AU in our model) for three scenarios: (1) Shown by the dashed-dotted line are model solutions with diffusive shock acceleration (Fermi-I) only. (2) The dashed line shows model solutions with diffusive shock acceleration and adiabatic heating and (3) the solid lines show model computations which include shock acceleration, heating in the inner he-

liosheath and acceleration of a stochastic nature (Fermi-II). For this scenario model solutions are shown at the shock (bottom solid line), at 100 AU (middle solid line) and at 120 AU (top solid line). In comparison the observations are shown. Note that the data points above 100 MeV/n are galactic cosmic rays which is not considered in this paper.

First, we concentrate on the computed anomalous spectrum at the termination shock assuming only diffusive shock acceleration to be present. This was done by setting $\nabla \cdot \vec{V} = 0$ beyond the shock and $D_0 = 0$ in Equation 2. The resulting computed intensity, $j \propto E^{-2.6}$ (where $j = P^2 f$) below 10 MeV and $j \propto E^{-3.6}$ thereafter. Note that the slope of the computed Fermi-I spectrum at the shock is dependent on the compression ratio s (which in our case is self-consistently computed from the flow profiles obtained with the hydrodynamic part of our model) and K_{rr}, the radial diffusion coefficient which determines the cutoff due to the curvature of the shock. Furhtermore, as illustrated by [18], both s and the injection efficiency of anomalous cosmic rays are depending on both latitude and solar cycle. [19] also illustrated that a changing K_{rr} as a function of latitude in the outer heliosphere results in a spectral break in the spectrum at the termination shock at low energies. When compared to Voyager 1 observations in Figure 1 the computed spectrum, assuming diffusive shock acceleration only, is steeper and also the observed upturn around 10 MeV is not present.

The dashed line in Figure 1 shows the computed spectrum at the shock, now including adiabatic heating of particles in the inner heliosheath. Compared to the case of diffusive shock acceleration only (dashed-dotted line), adiabatic heating results in a hardening of the spectrum at the shock with $j \propto E^{-2.3}$ for $E \leq 20$ MeV and $j \propto E^{-3.4}$ for $E \geq 20$ MeV. This is because particles are accelerated to higher energies resulting in lower spectral index. However, as illustrated by [7], the total effect of adiabatic heating is strongly related to K_{rr}. A smaller K_{rr} results in particles being heated to higher energies. When compared to the observations the computed spectrum below 10 MeV is more realistic when heating is included, but the observed upturn above $\sim$ 10 MeV is still not present.

It was also shown by [20, 21] that adiabatic heating of particles were necessary to reproduce the correct spectral shape at the shock. However, to simulate an upturn in the spectra a significant latitudinal dependent compression ratio were necessary. Furthermore, the source at the shock also needed to be significantly enhanced in the equatorial regions compared to other latitudes. Assuming this they were able to reasonably reproduce the Voyager 1 observations at the shock. We will illustrate next that apart from adiabatic heating additional acceleration in the inner heliosheath in the form of Fermi-II offer a more elegant way of explaining the Voyager 1 observations, in particular the observed upturn.

The solid lines in Figure 1 show model solutions at the shock (93 AU) and at 100 AU and 120 AU, including all three mentioned acceleration processes. Shown here is that at lower energies ($<$ 10 MeV) stochastic acceleration has no additional effect on the spectral slope at the shock compared to the previous case, similar to what [10] found. As will be shown later, this is not the case closer to the heliopause where stochastic acceleration becomes more effective, because of the dependence of this process on the Alfven speed and on $K_{||}$. When $K_{||}$ reduces abruptly over the shock and into the inner heliosheath because of the compression of the heliospheric magnetic field, and because the Alfven speed increases considerably toward the heliopause, stochastic acceleration is enhanced in this region.

Most important in Figure 1 is the flattening in the computed intensities between 10-30 MeV at the shock, a prominent observed feature. As ilustrated by the spectra at 100 and 120 AU this upturn at the shock results from anomalous particles being stochastically accelerated further out closer to the heliopause and then getting modulated on their way in. We thus find that our model, together with the choice of parameters as discussed above, results in realistic spectra at the shock.

Of special interest in Figure 1 is the large radial dependence of the computed intensities from the shock toward the heliopause for energies between 5 and 50 MeV. Shown here is that at e.g. $\sim$ 10 MeV a factor of $\sim$ 40 increase occurs from the shock to 120 AU. This is because of the unfolding of the computed spectrum closer to the heliopause with a significant reduction of the spectral index at energies below $\sim$ 20 MeV. This means that as

Voyager 1 will move toward the heliopause a significant increase in the intensities at these energies are predicted. However, as will be illustrated next, both diffusive, stochastic and adiabatic acceleration are sensitive to changes in the diffusion parameters. The question is open how these coefficients change spatially and over a solar cycle in the inner heliosheath.

Acknowledgements

We wish to thank H Moraal, R Caballero-Lopez, H Fichtner and J Snyman for valuable discussions. The authors are grateful for partial financial support granted to them by the South African NRF and the Deutsche DFG in the frame of the project "Heliocauses' (FI 706/6-1), and by the Meraka Institute as part of the funding for the South African CHPC.

References

[1] E. C. Stone, A. C. Cummings, F. B. McDonald, B. C. Heikkila, N. Lal, W. R. Webber, Science 309 (2005) 2017–2020.

[2] W. R. Webber, Journal of Geophysical Research (Space Physics) 110 (2005) 10103–+.

[3] M. S. Potgieter, Advances in Space Research (2007) in press.

[4] H. J. Fahr, T. Kausch, H. Scherer, Astron. Astrophys. 357 (2000) 268–282.

[5] V. Florinski, G. P. Zank, J. R. Jokipii, E. C. Stone, A. C. Cummings, Astrophys. J. 610 (2004) 1169–1181.

[6] U. W. Langner, M. S. Potgieter, H. Fichtner, T. Borrmann, Journal of Geophysical Research (Space Physics) 111 (2006) 1106–+.

[7] S. E. S. Ferreira, M. S. Potgieter, K. Scherer, Astrophys. J. 642 (2007) ***–***.

[8] R. Kallenbach, M. Hilchenbach, S. V. Chalov, J. A. Le Roux, K. Bamert, Astron. Astrophys. 439 (2005) 1–22.

[9] L. A. Fisk, G. Gloeckler, Astrophys. J. Lett. 640 (2006) L79–L82.

[10] M. Moraal, R. A. Caballero-Lopez, K. G. McCracken, F. B. McDonald, R. A. Mewaldt, V. Ptuskin, M. E. Wiedenbeck, in: J. Heerikhuisen, V. Florinski, P. Zank, N. V. Pogorelov (Eds.), AIP Conf. Proc. 858: Physics of the inner heliosheath: 5th Annual IGPP International Astrophysics Conference, 2006, pp. 219–225.

[11] M. Zhang, in: J. Heerikhuisen, V. Florinski, P. Zank, N. V. Pogorelov (Eds.), AIP Conf. Proc. 858: Physics of the inner heliosheath: 5th Annual IGPP International Astrophysics Conference, 2006, pp. 226–232.

[12] K. Scherer, H. Fichtner, B. Heber, S. E. S. Ferreira, M. S. Potgieter, Advances in Space Research (2007) in press.

[13] K. Scherer, S. E. S. Ferreira, Astrophysics and Space Sciences Transactions 1 (2005) 17–27.

[14] S. E. S. Ferreira, K. Scherer, Astrophys. J. 642 (2006) 1256–1266.

[15] E. N. Parker, Planet. Space Sci. 13 (1965) 9–49.

[16] R. Schlickeiser, Cosmic ray astrophysics / Reinhard Schlickeiser, Astronomy and Astrophysics Library; Physics and Astronomy Online Library. Berlin: Springer. ISBN 3-540-66465-3, 2002, XV + 519 pp., 2002.

[17] F. B. McDonald, E. C. Stone, A. C. Cummings, W. R. Webber, B. C. Heikkila, N. Lal, Geophys. Res. Lett. 34 (2007) 5105–+.

[18] K. Scherer, S. E. S. Ferreira, M. S. Potgieter, H. Fichtner, in: J. Heerikhuisen, V. Florinski, P. Zank, N. V. Pogorelov (Eds.), AIP Conf. Proc. 858: Physics of the inner heliosheath: 5th Annual IGPP International Astrophysics Conference, 2006, pp. 20–26.

[19] U. W. Langner, M. S. Potgieter, Advances in Space Research (2007) in press.

[20] U. W. Langner, M. S. Potgieter, in: J. Heerikhuisen, V. Florinski, G. P. Zank, N. V. Pogorelov (Eds.), AIP Conf. Proc. 858: Physics of the Inner Heliosheath, 2006, pp. 233–238.

[21] M. D. Ngobeni, M. S. Potgieter, Advances in Space Research (2007) in press.